

SYNTHESIS AND TRANSPORT STUDIES OF NANO-CRYSTALLINE $\text{Ce}_{1-x}\text{Bi}_x\text{O}_{2-\delta}$ SYSTEMS

Siomara Martinez-Costilla¹, Sagrario M. Montemayor¹, Padmasree Karinjilottu Padmadas²,
Antonio F. Fuentes²

¹Facultad de Ciencias Químicas, Universidad Autónoma de Coahuila, V. Carranza esq. J.
Cárdenas s/n, Saltillo, Coahuila, México, 25280

²Centro de Investigaciones Avanzadas del IPN, Unidad Saltillo, Carretera Monterrey-Saltillo Km.
13, Ramos Arizpe, Coahuila, México, 25900.
Contact e-mail: padma512@yahoo.com

ABSTRACT

In this work, a series of nano-crystalline solid solutions $(\text{CeO}_2)_{1-x}(\text{Bi}_2\text{O}_3)_x$ (where $0 \leq x \leq 1$, in steps of 0.2) were synthesized by Pechini method. The polymeric precursors were characterized by fourier transform infra red (FTIR) spectroscopy, and differential thermal analysis (DTA) and thermogravimetric analysis (TGA). The obtained solid solutions were studied by x-ray diffraction (XRD) and impedance spectroscopy (IS). All the prepared solid solutions exhibit a single phase cubic fluorite structure and the average crystallite size calculated using the Scherrer formula from the XRD spectra of all compositions treated from 400 to 800 °C were between 5.4 and 19.9 nm. Oxygen ion conductivity increased with the increase of dopant concentration and maximum is obtained for $\text{Ce}_{0.4}\text{Bi}_{0.6}\text{O}_{2-\delta}$ system. The Bi^{3+} doped ceria exhibit an ionic conductivity of the order of 10^{-3}S/cm at 600°C and is due to the presence of more oxygen vacancies introduced into the system with doping.

Keywords: Oxides, Electrolytes, Pechini method, Ionic conductivity

1. INTRODUCTION

Oxide ion conductors have been studied with great interest because of their various applications such as electrochemical devices, catalysis, sensors and in various optical materials [1]. Solid

oxide electrolyte is the main component of solid state electrochemical devices such as solid oxide fuel cells, oxygen sensors, oxygen pumps etc. Out of these, solid oxide fuel cells (SOFC) have attracted much attention because of their high efficiency and environmental friendliness. Currently yttria stabilized zirconia has been studied as the most reliable solid electrolyte for solid oxide fuel cell applications, but its high operating temperature causes many harsh effects on its performance. This leads to the search of other electrolytes based on CeO_2 , LaGaO_3 and Bi_2O_3 as alternatives to yttria stabilized zirconia which work at lower operating temperature. Doped ceria is the most promising high conducting solid electrolyte for low temperature SOFCs applications. Ceria has been successfully doped with many elements like Ca^{2+} , Y^{3+} , La^{3+} , Gd^{3+} , Sm^{3+} etc, but Bi^{3+} doped ceria system is interesting because of its high ionic conductivity and low operating temperature. CeO_2 doped with Bi_2O_3 are expected to form new electrolyte materials with better electrochemical properties because ceria doped with lower valence ions usually possess high oxide ion conductivity higher than yttria stabilized zirconia [2]. The structural similarity between cubic ceria and bismuth help to form solid solutions with the introduction of Bi into the CeO_2 lattice and is believed to be due to the formation of oxygen vacancies. This system might be of great interest for catalytic applications and integration in gas sensors. Several powder synthesis methods have been used in the preparation of ceria based electrolytes. Studies showed that the possibility of obtaining single phase $\text{CeO}_2\text{-Bi}_2\text{O}_3$ solid solution depend on the synthesis process [3]. Hydrothermal synthesis seems to be a good route for the synthesis of nanostructured ceria-bismuth system [4] but high temperature ceramic route failed to obtain the solid solution [5]. These methods have limitations due to its harsh synthesis conditions like high temperature, long reaction time etc. Pechini method has shown to be an important powder processing technique to produce complex oxide ceramics [6]. Some advantages of this route are: more homogeneity, fewer impurities, higher surface areas, lower crystal size and, especially, a good control in the stoichiometry. Although there are some studies which use citric acid and metallic nitrates as precursors [7] is important to notice that in this work, unlike the reported, the values of doped are from 0 to 1. The aim of this work is to synthesis $\text{Ce}_{1-x}\text{Bi}_x\text{O}_{2-\delta}$ (where $0 \leq x \leq 1$, in steps of 0.2) solid solutions by Pechini method and the polymeric precursors were characterized by FTIR and

DTA/TGA techniques and the obtained solid solutions were studied by x-ray diffraction and impedance spectroscopy.

2. EXPERIMENTAL PART

$\text{Ce}_{1-x}\text{Bi}_x\text{O}_{2-\delta}$ (where $0 \leq x \leq 1$, in steps of 0.2) solid solutions were prepared by Pechni method. The precursor gels were obtained using citric acid, ethylene glycol, $\text{Ce}(\text{NO}_3)_4 \cdot \text{H}_2\text{O}$ (99.9%), and $\text{Bi}(\text{NO}_3)_3 \cdot 5\text{H}_2\text{O}$ (99.9%). According to the stoichiometry of doped ceria, the appropriate quantities of nitrate were added to a homogeneous mix of citric acid and ethylene glycol. After stabilizing for 24 hours the solution was slowly dehydrated in an oven for 72 hours leading to a light yellow brittle film. The film was characterized by FTIR and thermal analysis by using Nicolet Magna IR Spectrometer 550 and TG/DTA Perkin Elmer Model Prys Diamon and then it is transferred to porcelain crucibles for heating in air at 400, 600 and 800°C for 2 hours. The resultant powders were characterized by XRD by using X-ray powder diffraction in Philips X'pert Diffractometer using Ni-filtered $\text{CuK}\alpha$ radiation ($\lambda = 1.5418 \text{ \AA}$). Specimens for electrical property measurements were pellets obtained by pressing the sample powder in a hydraulic press at a pressure of 5MPa with a diameter of 10 mm diameter and ~ 1 mm thickness. The pellets were placed in a platinum crucible and sintered at 700°C for 3 h in air with a slow heating rate of 2°C/minute. The two electrodes were formed by applying platinum paste to either surface of the pellets and then heat treated at 600°C for two hours before the measurement to burn out the binder of the platinum paste and to ensure good contact of the electrodes with the pellet. The transport properties of the sintered pellets were examined by ac impedance spectroscopy over a frequency range 100Hz to 1MHz using Solartron 1260 Frequency Response Analyzer in the temperature range 200-700°C.

3. RESULTS AND DISCUSSION

Figure 1 show the FTIR spectrum obtained for $\text{Ce}_{0.6}\text{Bi}_{0.4}\text{O}_{2-\delta}$ precursor as an example for all the spectra collected from other studied samples. FTIR spectra of precursors show that all the bands

associated to the ester groups present in the film as a consequence of the condensation reactions between citrate complexes and ethylene glycol. All the spectra contain a broad band at $\sim 3400\text{ cm}^{-1}$ due to the O-H stretching modes of the hydroxyl groups in the precursors and to the intermolecular hydrogen bonds. In addition, there are two bands related to C=O and C-O stretching vibrations of the ester groups at ~ 1730 and $\sim 1088\text{ cm}^{-1}$, respectively. The broad signal at 1606 cm^{-1} and that thin at 1380 cm^{-1} are associated to the ester groups which are coordinated to metallic ions. It is important to mention that these results are strongly supported on NMR analyses which will be reported in a future and that similar results were reported for systems with other metallic ions [8].

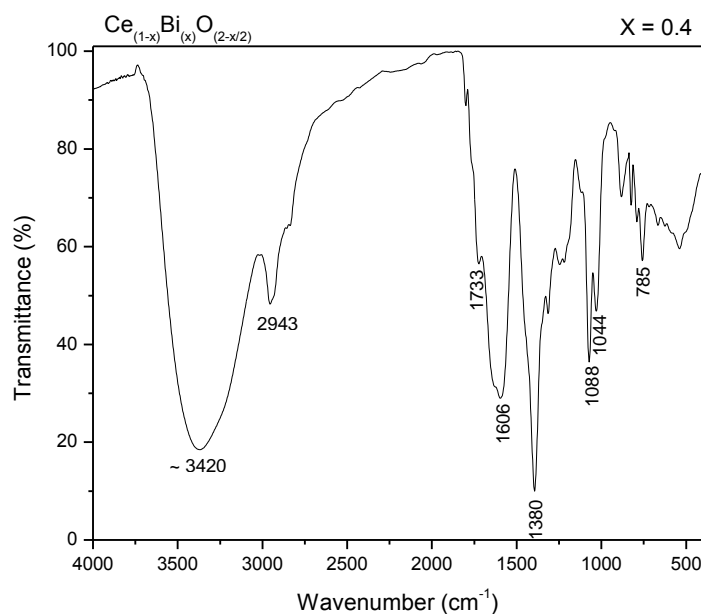


Figure 1. FTIR spectrum collected of $\text{Ce}_{0.6}\text{Bi}_{0.4}\text{O}_{2.8}$ precursor film

Thermal behavior of the precursor film was studied simultaneously by DTA/TG analysis. Figure 2 shows the DTA/TGA spectra obtained for the precursor $\text{Ce}_{0.4}\text{Bi}_{0.6}\text{O}_{2.8}$. Typically the samples lose weight gradually as the temperature increases from room temperature to $\sim 350\text{ }^{\circ}\text{C}$ through one endothermic event, between ~ 50 and $\sim 110\text{ }^{\circ}\text{C}$, and two exothermic events, at ~ 130 and $\sim 350\text{ }^{\circ}\text{C}$. The broad endothermic peak can be attributed primarily due to the dehydration of

the film whereas the exothermic peaks probably correspond to the burning of the organic matter in the sample and to the gradual crystallization process of the $\text{Ce}_{1-x}\text{Bi}_x\text{O}_{2-\delta}$. Above 400 °C there are no considerable changes.

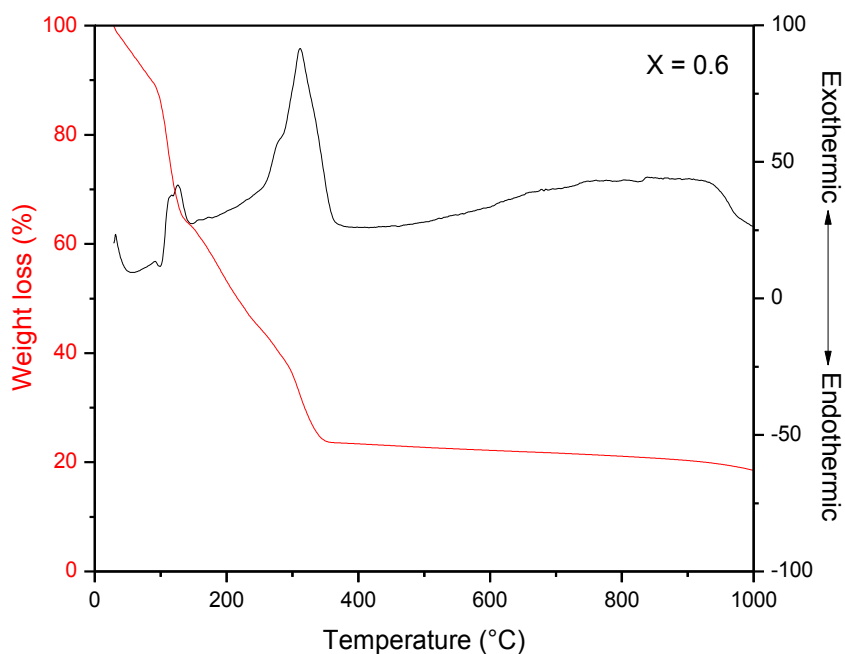


Figure 2. DTA/TG curves obtained from $\text{Ce}_{0.4}\text{Bi}_{0.6}\text{O}_{2-\delta}$ precursor film.

Figure 3 shows the XRD pattern obtained for $\text{Ce}_{0.2}\text{Bi}_{0.8}\text{O}_{2-\delta}$ sample treated at 400 and 800 °C by 2 hours. Thermal treatments at the low temperature of 400 °C, by two hours, lead to obtain a fluorite-phase in all compositions studied. Although the peaks are broader and of lower intensity than those of well crystallized CeO_2 , the reduction in the temperature is very significant when it is compared with traditional solid state techniques. An increase in the temperature of the thermal treatments permits that the half-width of peaks becomes narrower and the intensity of them gets stronger, as shown in Figure 3. The average crystallite size, D , of bismuth substituted ceria powders, calculated using the Scherrer formula from XRD of all compositions treated from 400 to 800 °C were between 5.4 and 19.9 nm. All the samples studied in this series have cubic

fluorite structures. With the increase of Bi content, a small shift of all reflections towards the lower angles was observed. The shift is more apparent for the higher bismuth content for the composition $\text{Ce}_{0.2}\text{Bi}_{0.8}\text{O}_{2-\delta}$, where 80% of the cerium atoms are replaced by the larger bismuth atom. The analysis of the crystallite size of the samples of this series shows the crystallite size varies between 16-19 nm when the Bi concentration changes from 20-80%.

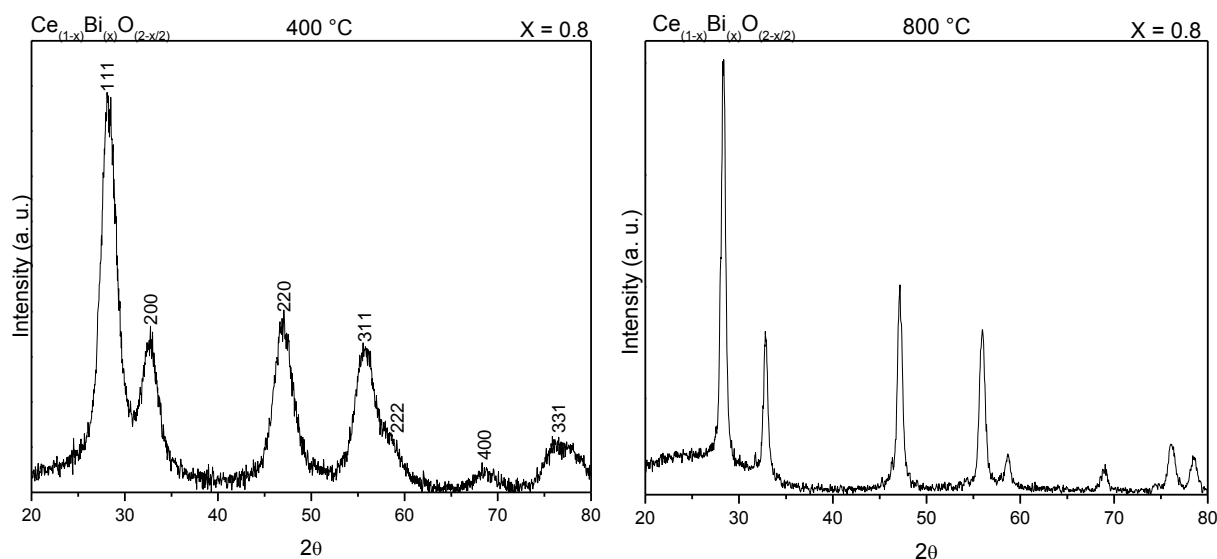


Figure 3. XRD patterns obtained from $\text{Ce}_{0.2}\text{Bi}_{0.8}\text{O}_{2-\delta}$ treated at 400 and 800 °C by 2 hours.

The electrical properties of the nanocrystalline ceria bismuth solid solutions were determined by impedance spectroscopy technique. Generally an impedance spectra consist of bulk, grain boundary and electrode polarization part. The intercept of the high frequency semicircle at the real axis represents the bulk resistance (R_b), the intercept of the intermediate frequency semicircle is the grain boundary resistance (R_{gb}) and the intercept of the low frequency semicircle is the electrode polarization resistance. Figure 4 shows the impedance spectra obtained for the solid solution $\text{Ce}_{0.6}\text{Bi}_{0.4}\text{O}_{2-\delta}$ at different temperatures. In the low temperature range, only one arc (the high frequency arc) is obtained and it corresponds to the bulk effect, whereas the grain boundary contribution is negligible at low temperature. From the figure we can see that with the increase of

temperature the resistance of the sample decreases. The conductivity at each temperature can be found out by the resistance obtained from the impedance spectra.

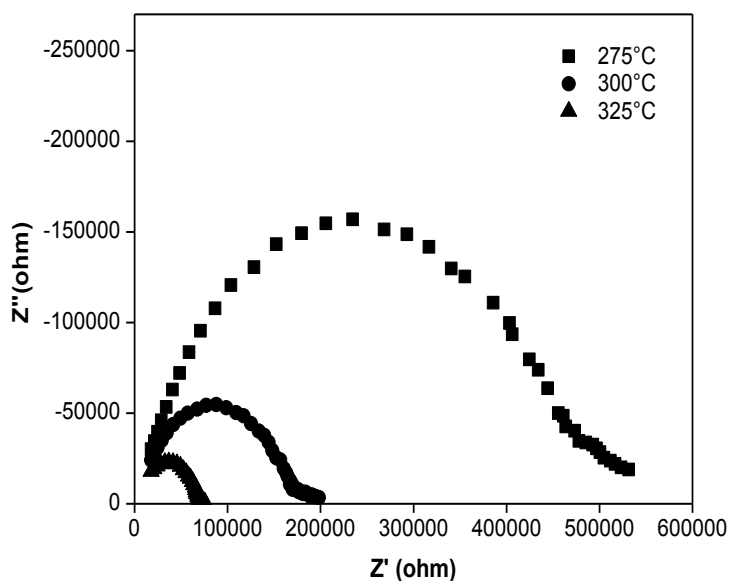


Figure 4. Impedance spectra obtained for the sample $\text{Ce}_{0.6}\text{Bi}_{0.4}\text{O}_{2-\delta}$ at different temperatures

The measured conductivity data were analyzed with the Arrhenius equation

$$\sigma = \sigma_0 \exp\left(-\frac{E_a}{kT}\right) \quad (1)$$

where E_a is the activation energy for ion migration, k is the Boltzman's constant, T is the absolute temperature and A is the pre-exponential factor being a constant in certain temperature range. The Arrhenius plot of the ionic conductivities for the sample $\text{Ce}_{1-x}\text{Bi}_x\text{O}_{2-\delta}$ (where $x=0, 0.4, 0.6, 1$) is shown in Figure 5. The electrical conductivity of $\text{Ce}_{1-x}\text{Bi}_x\text{O}_{2-\delta}$ increases with the increase in bismuth doping and reaches a maximum for the composition $\text{Ce}_{0.4}\text{Bi}_{0.6}\text{O}_{2-\delta}$. The conductivity varies linearly at temperatures below 500°C and above that temperature a significant bending which is usually interpreted as a transition from associated to dissociated behavior of the defect

cluster or complex. That is in the low temperature region; the activation energy equals to the migration enthalpy and defect association enthalpy and in the high temperature region is associated with only the migration enthalpy [10]. Similar behavior was reported for ceria [11] and

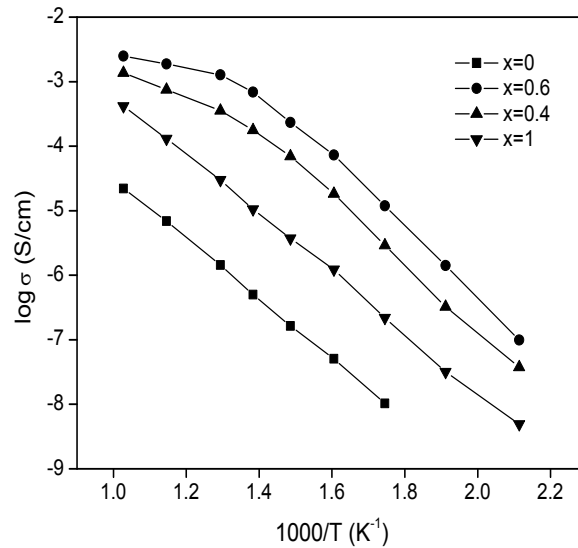
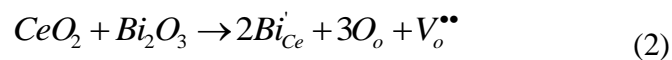


Figure 5. Temperature dependence of conductivity for the sintered solution $\text{Ce}_{1-x}\text{Bi}_x\text{O}_{2-\delta}$

and LaGaO_3 [12] based oxides. Pure ceria is a poor oxide ion conductor. The ionic conductivity increased considerably when Ce^{4+} is replaced by Bi^{3+} because of the introduction of oxygen vacancies and it can be represented by the Kröger-Vink notation as



where $\text{Bi}_{\text{Ce}}^{\cdot}$ represents Bi^{3+} ion in the Ce^{4+} sites, O_o represents O^{2-} ions on a regular oxygen lattice site, and $\text{V}_o^{\bullet\bullet}$ represents oxygen vacancies. The change observed at around 500°C can be explained by the changes in the behaviors of the defects in this doped ceria system. In the low temperature range, the oxygen vacancy associated with the dopant is trapped as a result of the association of defects to form defect complexes. Consequently, both the association energy and the migration energy of the system influence the conduction mechanism. At high temperatures,

mostly all oxygen vacancies are free and the bulk conductivity is determined by the oxygen ion migration. Table 1 shows the bulk conductivity and activation energies obtained for the nanocrystalline $\text{CeO}_2\text{-Bi}_2\text{O}_3$ solid solutions sintered at 700°C . The highest ionic conductivity ($\sigma_b=2.48 \times 10^{-3}\text{S/m}$) is obtained for the $\text{Ce}_{0.6}\text{Bi}_{0.4}\text{O}_{2-\delta}$ system out of all studied samples.

Table 1. Conductivity (σ_b) and activation energies (E_a) for the bulk conduction in the nano-crystalline solid solutions $\text{CeO}_2\text{-Bi}_2\text{O}_3$ sintered at 700°C

Solid Solutions	$\sigma_b(\text{S/cm})$ (600°C)	E_a (eV)	Temperature range
$\text{Ce}_{1.0}\text{Bi}_{0.0}\text{O}_{2-\delta}$	2.21×10^{-5}	0.923	300-700
$\text{Ce}_{0.6}\text{Bi}_{0.4}\text{O}_{2-\delta}$	1.36×10^{-3}	1.049	200-450
$\text{Ce}_{0.4}\text{Bi}_{0.6}\text{O}_{2-\delta}$	2.48×10^{-3}	1.032	200-450
$\text{Ce}_{0.0}\text{Bi}_{1.0}\text{O}_{2-\delta}$	4.15×10^{-4}	0.913	200-700

4. CONCLUSIONS

The Pechini method is an excellent route for the synthesis of bismuth doped ceria leading to single phase fluorite-type structures, in the entire solid solution. The low temperature necessary for obtaining may be due to the high homogeneity of the precursors used were there are two types of reactions, complexation and esterification. The average crystallite size of bismuth substituted ceria powders, calculated using the Scherrer formula from the XRD spectra of all compositions treated from 400 to 800°C were between 5.4 and 19.9 nm. The conductivity increased with the increase of dopant concentrations and a maximum conductivity is obtained for $\text{Ce}_{0.6}\text{Bi}_{0.4}\text{O}_{2-\delta}$ system.

REFERENCES

- [1] L. Li and B. Yan, *J. Non-Crystalline Solids*, **355**, 776-779 (2009).
- [2] P. Shuk, H.-D. Wiemhofer, U Guth, W. Gopel, M. Greenblatt, *Solid State Ionics*, **89**, 179-196 (1996).
- [3] Z. Li, H. Zhang, B. Bergman, *Ceram. Inter.*, **34**, 1949-1953 (2008).

- [4] X.L. Chen, W. Eysel, *J. Solid State Chem.*, **127**, 128-130 (1996).
- [5] G.S.Li, L.P. Li, S.H. Feng, M.Q. Wang, L.Y. Zhang, X. Yao, *Adv. Mater.*, **11**, 146-149 (1999).
- [6] C. Peng, Y. Zhang, Z. W. Cheng, X. Cheng, J. Meng, *Journal of Materials Science: Materials in Electronics*, **13**, 757-762 (2002).
- [7] H. Yao, Y. Zhang, J. J. Liu, Y. Li, J. Wang, Z. Li, *Materials Research Bulletin*, **46**, 75-80 (2011).
- [8] S. M. Montemayor, L. A. García-Cerda, J. R. Torres-Lubián, *Materials Letters*, **59**, 1056-1060 (2005).
- [10] N Cioatera, V. Parvulescu, A. Rolle, R.N. Vannier, *Solid State Ionics*, **180**, 681-687 (2009).
- [11] B. Li, Y. Liu, Xi Wei, W. Pan, *J. Power Sources*, **195**, 969-976 (2010)
- [12] K Huang, R S Tichy, J B Goodenough, *J Am.Ceram. Soc.*, **81**, 2565-2575(1998).